Meso- and Microscale Features of a Colorado Cold Front

GEORGE S. YOUNG AND RICHARD H. JOHNSON

Department of Atmospheric Science, Colorado State University, Fort Collins, CO 80523

(Manuscript received 20 December 1983, in final form 1 June 1984)

ABSTRACT

Data from the NOAA BAO (Boulder Atmospheric Observatory) tower and the PROFS (Program for Regional Observing and Forecasting Services) surface mesonetwork have been used to detect the meso- and microscale flow patterns associated with the passage of a shallow cold front over complex terrain. This front moved across the PROFS surface mesonetwork and the BAO tower site on the morning of 3 December 1981. Partial blocking of the cold airflow by the higher terrain to the north led to a westward movement of the cold front in the upper reaches of the South Platte River drainage basin. A meso-β-scale anticyclonic eddy subsequently formed in the lee of this terrain obstruction.

The micro-α-scale vertical eddy structure in the cold frontal zone is defined using data from the BAO tower. Updrafts of >6 m s^{-1} at 200 m AGL occurred at the wind-shift and temperature-drop line. Immediately behind this feature, micro-α-scale eddies entrained air through the frontal surface, diluting the low-level flow which was overtaking the front from behind. These features have been observed by others in atmospheric and laboratory gravity currents.

1. Introduction

This study uses new data to expand the preliminary results of Shapiro (Anthes, 1983), who has studied mesoscale orographic interactions with cold fronts over northeast Colorado. Two scales of eddy motion associated with a 3 December 1981 cold front passage across the upper reaches of the South Platte River drainage basin in northeast Colorado will be discussed. First, the meso-β-scale (Orlanski, 1975) motions resulting from the flow of the cold air mass around a ridge which borders this basin will be documented using data from the PROFS (Program for Regional Observing and Forecasting Services; Reynolds, 1983) surface mesonetwork. Second, the micro-α-scale structure of the cold front head and the structure of vertical eddies within it will be defined using data from the NOAA BAO (Boulder Atmospheric Observatory) tower.

Previous studies of flow around elevated terrain features have generally been limited to case studies of lee mesocyclones and convergence zones or to satellite observations of vortex streets in maritime stratocumulus clouds. Reed (1980) and Smith (1981) discuss the mesoscale flow around the Olympic mountains which led to the destruction of the Hood Canal bridge in the state of Washington. In the same region, Mass (1981) described the more frequent but less severe case of mesoscale convergence zones. These topographically induced convergence zones appear to have a structure similar to that of shallow cold fronts. Chopra and Hubert (1964, 1965), Lyons and Fujita (1968), Tsuchiya (1969) and Zimmerman (1969), using satellite images of stratocumulus decks, have studied the vortex streets shed by islands. These studies indicate that the boundary-layer flow will deflect around terrain obstructions if it is capped by a layer of sufficient static stability which is located below the top of the obstruction. Similar deflection of the boundary-layer airflow and formation of a lee eddy are observed in this study of the interaction of a shallow cold front with a ~500 m high ridge.

The fine structure of gravity currents has been studied for a variety of atmospheric and laboratory flows. Clarke (1961), Browning and Harrold (1970), Martin (1973), Carbone (1982), Hobbs and Persson (1982) and Parsons and Hobbs (1983) used a variety of sensors including Doppler radar, serial pibals, rawinsondes, aircraft and surface observations to study the fine structure of cold fronts. The temporal and vertical resolution of available data limited the amount of frontal structure detail obtainable from these studies. Despite these instrument limitations, Martin (1973) was able to document large temperature decreases within the first 10 s of frontal passage and the existence of pockets of air residing at the surface behind the front which had wind and temperature characteristics of the prefrontal air mass. The present study confirms Martin's hypothesis that these pockets can result from entrainment through the frontal surface by vertical eddies. Browning and Harrold (1970), Carbone (1982), Hobbs and Persson (1982) and Parsons and Hobbs (1983) all report strong updrafts along the leading edges of moist cold fronts which are similar to those observed in the 3 December 1981 case.

The structure of vertical cross sections of thunderstorm gust fronts has been studied using radar, mesoscale surface networks and instrumented towers. Charba (1974) and Goff (1976) both report updrafts of ~ 5 m s^{-1} within the gust front zone near the location of the first temperature drop. The observed features of thunderstorm gust fronts are generally similar to those reported for cold fronts by the authors cited above.

Gravity currents observed in laboratory tank experiments have many features in common with atmospheric gravity currents (Simpson, 1979). In particular, roll eddies are observed to mix fluid through the frontal surface. The structure and effects of these eddies are quite similar to those observed on the frontal surface in the 3 December 1981 case.

A detailed comparison of the methods and results of this and previous studies is presented in Section 4.

2. Data sources

a. PROFS mesonetwork

Surface observations from a mesometeorological network of 22 stations over northeast Colorado have been used in our analysis. A map of these stations (small letters) and the surrounding National Weather Service (NWS) stations (large letters) is shown in Fig. 1. The separation between PROFS stations is variable, but averages about 40 km. Standard meteorological variables are recorded and transmitted in the form of 5-minute averaged data. A listing of the stations, identifiers and elevations of the PROFS mesonetwork stations in Fig. 1 is given in Table 1. Major topographic features of the region are also indicated in Fig. 1. The PROFS stations are centered over the upper reaches of the South Platte River drainage basin with the Continental Divide on the west, the Cheyenne Ridge to the north and the Palmer Lake Divide to the south.

b. BAO tower

Observations from the 300 m instrumented tower of the NOAA BAO (Kaimal and Gaynor, 1983) have been used in our analysis of the micro-α-scale features of the cold frontal zone. The BAO tower is located near 40°N, 25 km east of the first foothills of the Front Range of the Rocky Mountains (Fig. 1). The tower instrumentation is described in detail by Kaimal and Gaynor (1983). For this study, all eight vertical levels (10, 22, 50, 100, 150, 200, 250 and 300 m) of the tower were used. Sonic anemometers provided u, v and w data in 0.05 Hz block averages. Quartz thermometers provided high accuracy temperature data with a 1-minute time constant. Less accurate but faster response platinum wire thermometers provided temperature data with a 5–10 Hz cutoff for the three levels at which they were operational. All data used were sampled at 0.1 Hz for this study.

3. Observations

a. Macroscale analysis

The 0000 GMT 3 December 1981 NMC (National Meteorological Center) surface analysis depicts a weak cold front extending from a low in northeastern Montana south into northern Wyoming and then west to the Pacific coast. Successive isochrones of NMC-analyzed frontal positions from 0000 to 1800 are presented in Fig. 2. As the cold front moved south and east, NMC dropped the section west of the Front Range of the Rocky Mountains. The front was analyzed by NMC to move southward across the eastern Colorado plains between 0600 and 1200 while maintaining a west-northwest to east-southeast orientation. The NMC 0900 surface analysis placed the front across the region covered by the PROFS mesonetwork in northeastern Colorado. Data from this network will be used to resolve the mesoscale features of the frontal motion in northeastern Colorado. The 1200 NMC surface chart (Fig. 3) depicts the macroscale setting in which the meso- and microscale flows described below are embedded. Inclusion of data from the PROFS mesonetwork into the analysis leads to cold frontal positions in eastern Colorado which are further north than those depicted in this NMC analysis (as will be evident from the following subsection).

b. Mesoscale analysis

Hourly surface charts for the PROFS mesonetwork are shown in Fig. 4. Subjectively-analyzed streamlines, frontal positions and temperature change fields are depicted. These mesoscale data show that the effects of terrain on the front are considerably more complex than those which can be resolved by the synoptic network used for the NMC surface analysis.

Prior to the passage of the cold front, all stations were experiencing warm northwesterly chinook flow. As the front passed, wind shifts occurred to a variety of directions dictated by mesoscale topographic influences. The western end of the front was held back by the Cheyenne Ridge at the northern border of the South Platte River drainage basin. The sections of the front beyond the east end of the Cheyenne Ridge proceeded south unimpeded, as evidenced by the higher frontal and wind speeds on the eastern plains. As this eastern section of the front progressed, the cold air mass entered the river basin from the northeast, around the end of the ridge. This flow around the end of the Cheyenne Ridge is shown for 1200 in Fig. 5. By 1200, three hours after the NMC-analyzed frontal passage across the PROFS mesonetwork, the cold air still had not reached the foothills of the Rocky Mountains. The cold front had passed BYE by 1100 yet by 1300 it had not yet passed FCL which is well to the north and at a similar elevation on the plains. Clearly, more than station elevation and dis-

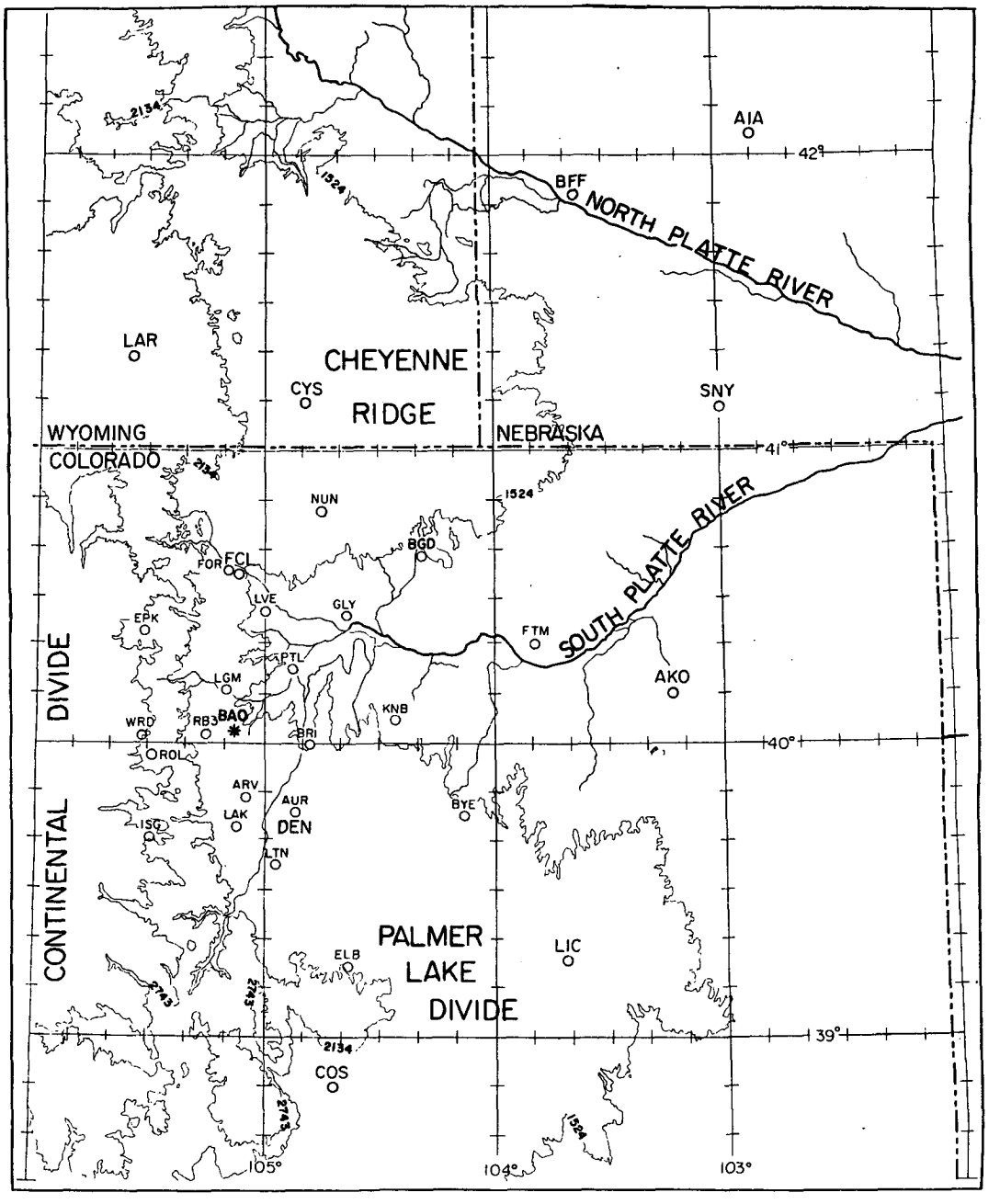

FIG. 1. PROFS mesonetwork stations (small letters), surrounding National Weather Service stations (large letters) and the BAO tower site. Major geographical features are identified. Elevation contours in meters.

tance to the south controlled the time of frontal passage: station location relative to the higher western portion of the Cheyenne Ridge was critical. The final equilibrium position of the front followed a terrain contour approximately equal in height to the top of the cold air mass.

During this time an anticyclonic eddy formed in the lee of the Cheyenne Ridge so that the cold front passage at FCL in the northwest corner of the basin was actually from the southeast. This eddy continued to expand southward with time until it filled the entire basin between the Cheyenne Ridge and the Palmer Lake Divide. This eddy differed from those observed in the wakes of islands in that it was not shed and reformed periodically. This steadiness may result from the influences of the Front Range of the Rocky Mountains to the west and the Palmer Lake Divide to the south.

TABLE 1. PROFS mesonetwork stations and their elevations.

Identifier	Name	Elevation (m)
ARV	Arvada	1643
AUR	Aurora	1625
RB3	Boulder	1609
BGD	Briggsdale	1483
BRI	Brighton	1518
BYE	Byers	1554
ELB	Elbert	2146
EPK	Estes Park	2377
FOR	Fort Collins	1609
FTM	Fort Morgan	1372
GLY	Greeley	1414
ISG	Idaho Springs	3505
KNB	Keenesburg	1521
LAK	Lakewood	1832
LIT	Littleton	1750
LGM	Longmont	1533
LVE	Loveland	1512
NUN	Nunn	1634
PTL	Platteville	1457
ROL	Rollinsville	2749
WRD	Ward	3048

It is interesting to note that while the PROFS surface report at the Denver airport (AUR) at 1200 (a five-minute average prior to that time) shows that the cold front had passed that location, the 1200 report from the National Weather Service station at the airport (Fig. 3; northwesterly wind, 9°C temperature) indicates that the front had *not* yet passed there. The discrepancy is explained by the fact that the National Weather Service 1200 report is based on an observation at a slightly earlier time (1145).

c. *Microscale analysis*

At 1137 the cold front (oriented approximately north–south) moved westward across the site of the BAO tower, providing an opportunity to study the fine structure within its head and frontal zone. Time–height sections of the component of wind perpendicular to the front, potential temperature and vertical velocity are examined and a description of the structure and eddy motions within the frontal zone is provided. Horizontal and vertical wind component data are only available until 1145. Temperature data are available for later periods and so will be depicted for the period ending at 1200 when the vertical profile of temperature ceases to change.

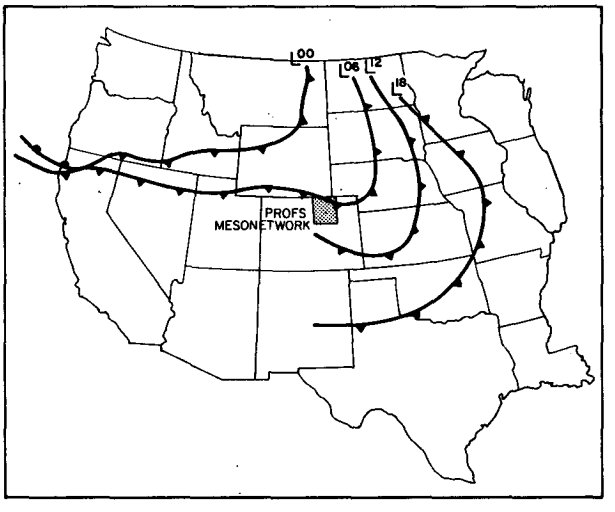

FIG. 2. Isochrones of the NMC-analyzed cold front position, 0000–1800 GMT 3 December 1981.

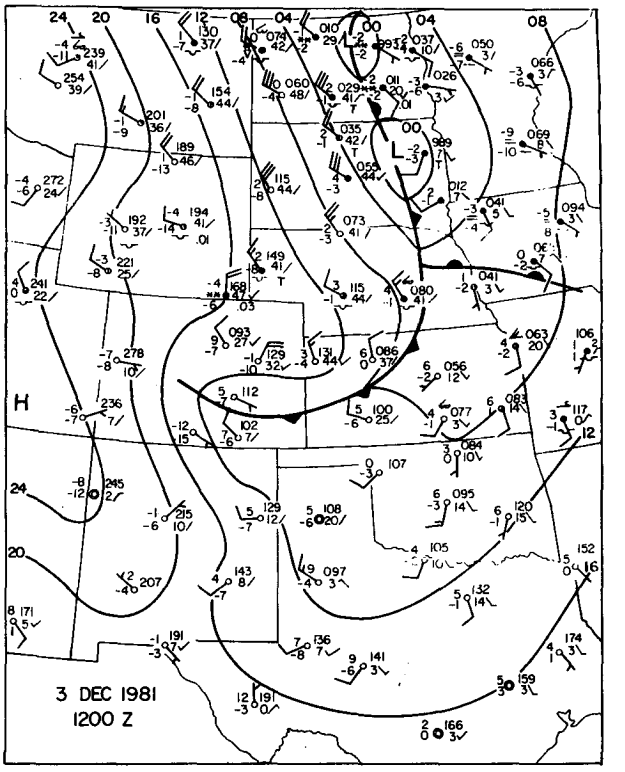

FIG. 3. NMC-analyzed surface chart, 1200 GMT 3 December 1981. Surface observations are plotted and analyzed according to the standard conventions with temperatures in °C and each full wind barb representing 5 m s^{-1} and each half barb 2.5 m s^{-1}.

The time–height section of the u-component of wind velocity (positive for westerly flow) at the tower is presented in Fig. 6. The frontal speed during this interval can be calculated from the PROFS mesonetwork data and is $\sim$10 m s^{-1}. Thus, one minute on a time–height section is approximately equivalent to 600 m in the direction perpendicular to the front. This time-to-space conversion is based on the steady state assumption. While the front itself is generally steady state on the time scales presented, the observed micro-α-scale structures are but one realization of a number of similar transitory phenomena.

Chinook flow with speeds at 300 m aproaching 20 m s^{-1} and a logorithmic wind profile (not shown) was occurring 0.5 h before the frontal passage. As the

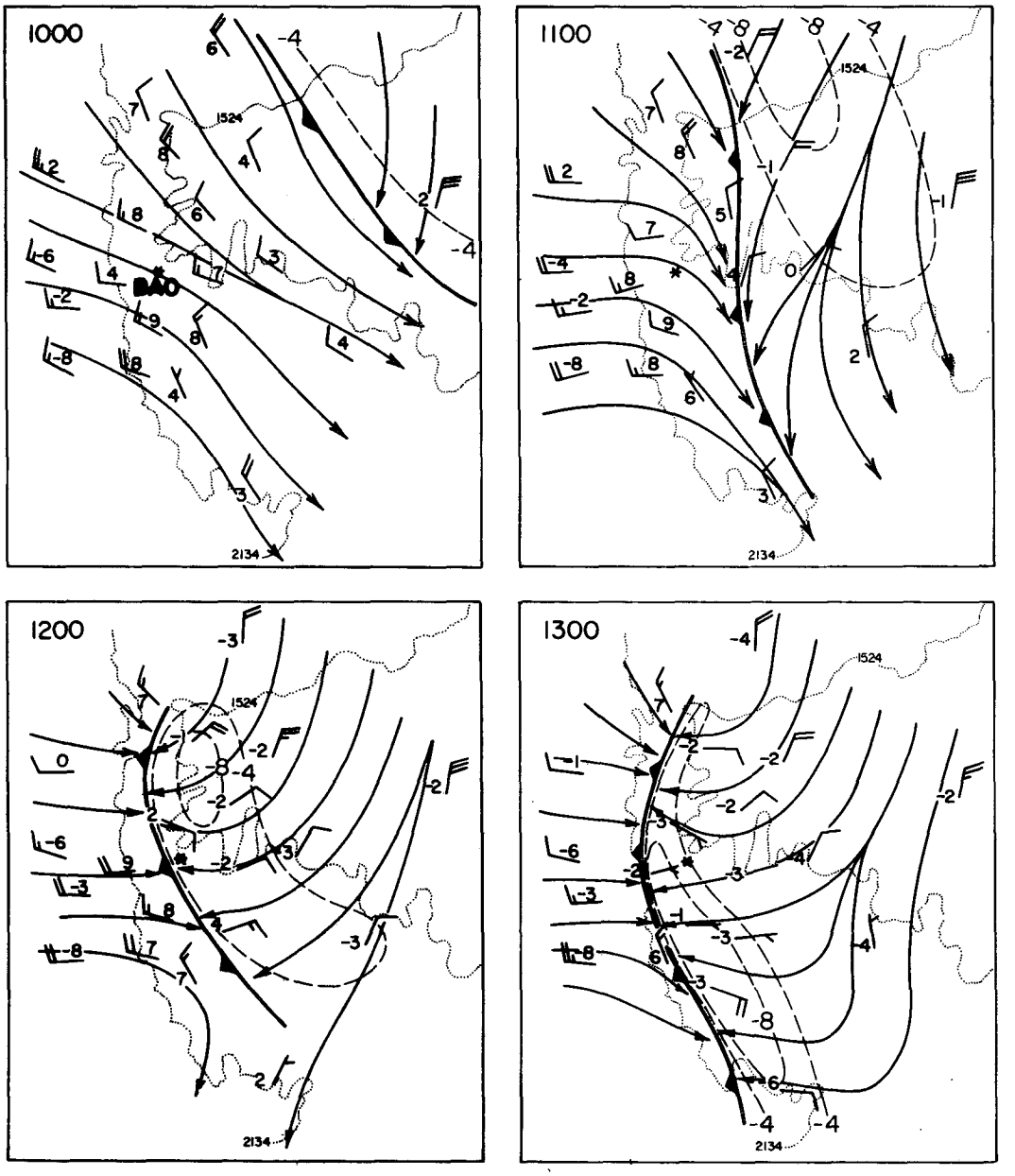

FIG. 4. Surface charts for the PROFS mesonetwork, 1000–1300 GMT 3 December 1981. The analysis region is depicted by shading in Fig. 2. Dashed lines denote temperature change during the previous hour (°C h^{-1}) and solid arrows follow streamlines of the flow. Topographic contours (m) are denoted by dotted lines. Surface wind and temperature are plotted for each PROFS station with units as in Fig. 3.

time of frontal passage approached, winds at all levels became light with a tendency for an easterly component below 200 m and a westerly component above. By 1136:50, the surface wind-shift line had reached the tower. Within 50 s the wind-shift line had reached the top of the tower at 300 m. This timing corresponds to a wind-shift line slope of ~30°.

Between 0.5 and 1.0 km behind the wind-shift line and below 200 m lies a vertical tongue of strong easterly winds. This tongue forms an upward extension of the layer of maximum horizontal wind which is centered at 50–100 m above the surface. Behind this tongue of strong winds is a region of weak winds extending downward from above the tower to within 50 m of the ground. At the tower top this region of weak winds extends from 1.4 to 2.4 km behind the surface frontal position, while at its lower limit it is centered at 1.2 km behind the surface frontal position. These features of the field of horizontal wind can be related to vertical circulations within the cold frontal

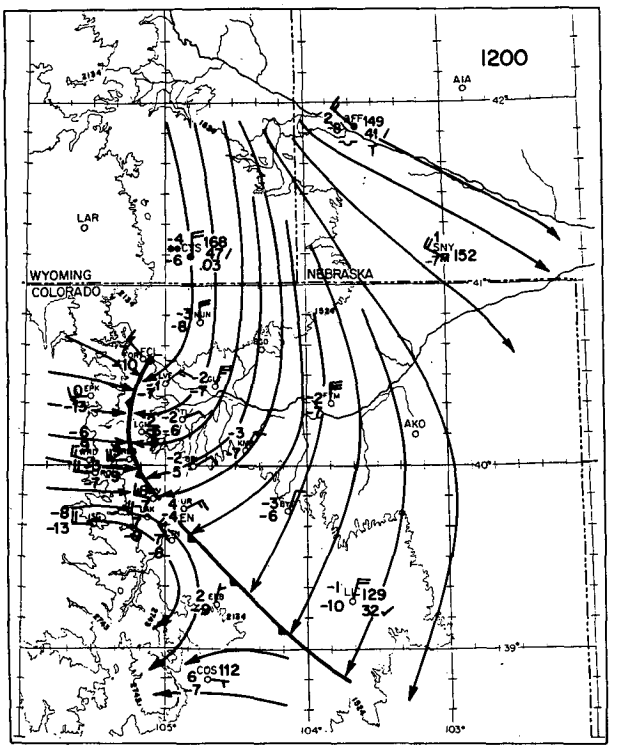

FIG. 5. Surface chart of the PROFS mesonetwork and surrounding synoptic network stations, 1200 GMT 3 December 1981. Solid arrows follow streamlines of the flow. Topographic contours (m) are denoted by thin solid lines.

head. Manifestations of these circulations also can be seen in time–height sections of potential temperature and vertical velocity.

A time–height section of potential temperature θ_G, where

$$\theta_G(z) = T(z) + \Gamma_d z,$$

is presented in Fig. 7 (z is height above ground and Γ_d the dry adiabatic lapse rate). The slow warming trend observed prior to frontal passage terminates by 1137:00 at the surface and by 1137:40 at 300 m. This timing corresponds to a cold front slope of ~36°. Following frontal passage there is a rapid temperature decrease at all levels. The one-minute time constant of the quartz thermometers leads to a considerable underestimate of the frontal zone temperature gradient. The fast response temperature data from the platinum wire thermometer at 250 m is presented in Fig. 8. The temperature decrease observed with this instrument is 3.6°C in the first 10 s followed by a further 2.0°C within the first minute after frontal passage. Following this decrease, there is a warming at the upper levels which lasts several minutes and reaches down with diminished amplitude to 100 m. Several similar episodes occur at later times. Each successive warming is of smaller amplitude and reaches less far down into the cold air mass. The axis of the cold air is observed at the 50 m level. The depth of the layer of cold air of weak static stability increases with time from 50 m at 1140 to 150 m at 1200.

Above this cold air is a layer in which potential temperature increases by ~5°C (100 m)$^{-1}$. After 1143, this stable stratification extends above the top of the tower. Extrapolating the potential temperature profile upward gives 400 m as an estimate of the height of the frontal surface at 1200.

The time–height section of vertical velocity is depicted in Fig. 9. These data allow an understanding of the structures seen in the other fields. Significant downdrafts existed in the slightly stable air ahead of the cold front. These downdrafts account at least in part for the observed warming at all levels. An updraft approximately 1 km wide is centered on the wind-shift line. The leading edge of the updraft is vertical while the trailing edge below 200 m slopes back at about the same angle as the frontal surface. The increase in updraft strength with height combined with this increase in width indicates that there is

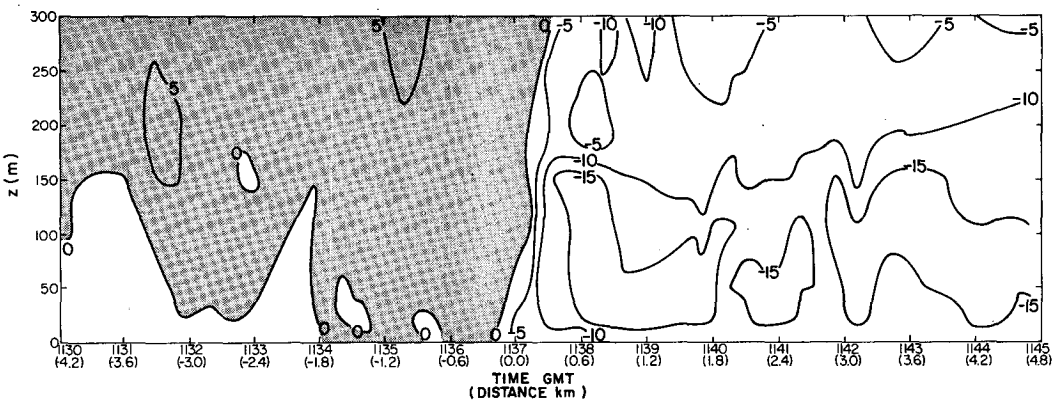

FIG. 6. Time–height section of the u-component of wind (m s^{-1}) for the BAO tower on 3 December 1981. Data are from eight sonic anemometers sampled at 0.1 Hz. The horizontal space scale is based on the assumption of steady translation at 10 m s^{-1}. The regions of winds with a component from the west are shaded.

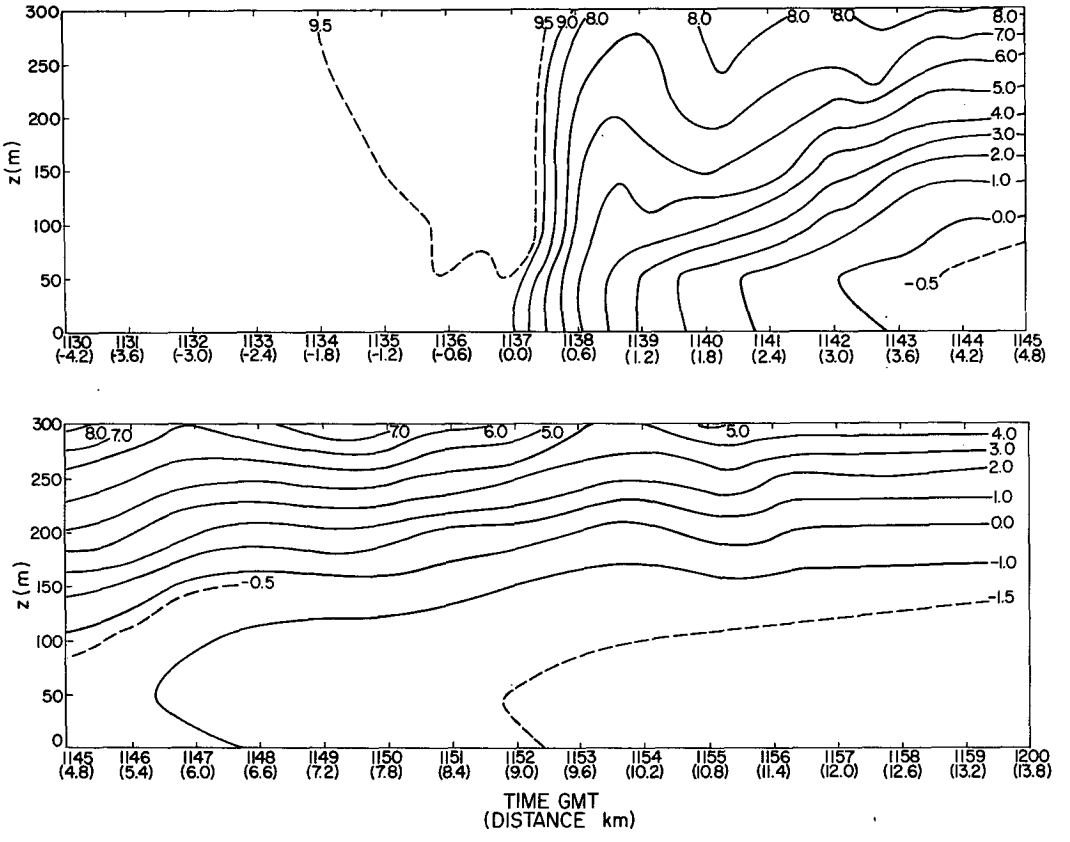

FIG. 7. Time–height section (upper and lower segments are sequential) of potential temperatures (°C) for the BAO Tower on 3 December 1981. Data are from eight quartz thermometers with time constants of one minute. The horizontal space scale is based on an assumption of steady translation at 10 m s^{-1}.

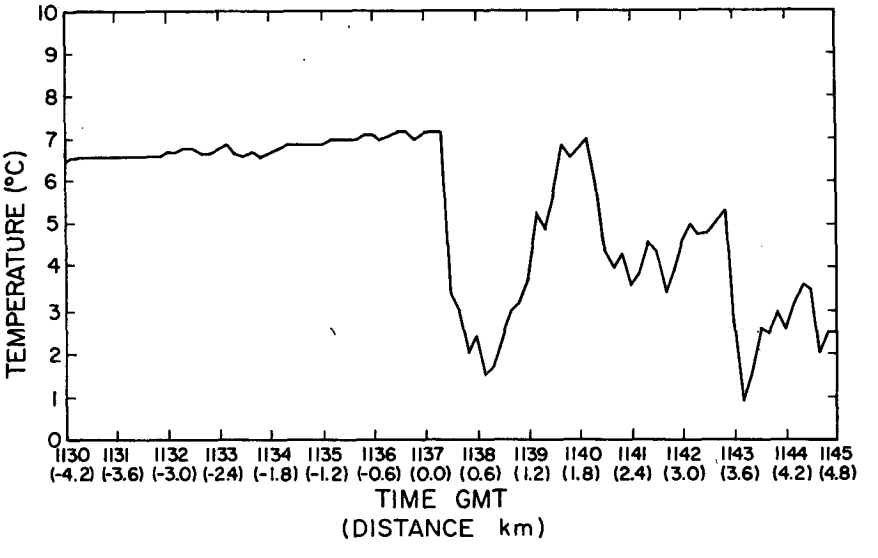

FIG. 8. Time section of fast-response temperature (°C) for the 250 m level of the BAO tower on 3 December 1981. Data are from the platinum wire thermometer with a 5–10 Hz cutoff sampled at 0.1 Hz. The horizontal space scale is based on an assumption of steady translation at 10 m s^{-1}.

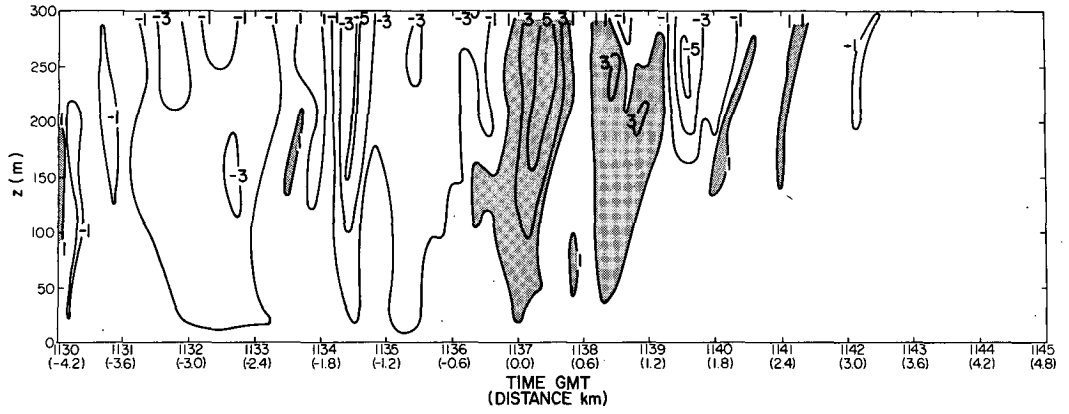

FIG. 9. Time–height section of the w component of wind (m s^{-1}) for the BAO tower on 3 December 1981. Data are from eight sonic anemometers sampled at 0.1 Hz. The horizontal space scale is based on an assumption of steady translation at 10 m s^{-1}. The regions of updrafts exceeding 1 m s^{-1} are shaded.

entrainment into the frontal updraft throughout the lowest 200 m. Maximum vertical velocities > 6 m s^{-1} are observed at 200 and 250 m.

Behind the wind-shift line is a second updraft corresponding in time to the vertical tongue of lowered potential temperature and enhanced wind speed. Behind this second updraft is a downdraft corresponding in time to the vertical tongue of elevated potential temperatures and decreased wind speeds. This pattern is repeated behind the initial eddy, with each successive eddy having smaller amplitude and less penetration into the cold air mass. These eddies resemble the breaking billows observed in frontal zones of laboratory gravity currents. A schematic diagram of the structure of the observed cold front head is provided in Fig. 10. The solid curves represent scalar quantities and the arrows indicate flow directions relative to the front. The primary features are the jet of relatively undiluted air overtaking the front from behind and a series of eddies mixing air down through the frontal zone and diluting the cold air mass from above. The updrafts are thus relatively cool and fast while the downdrafts are relatively warm and slow. The vertical eddies in this study behave like those hypothesized by Martin (1973) from his study of surface data. In this case study, however, the eddies did not penetrate to the surface.

4. Comparison with previous studies

a. Mesoscale structures

Previous studies have described a number of mesoscale flow structures associated with flow around terrain features. There have also been numerous studies of the mesoscale features of macroscale cold fronts. The methods and results of these studies will be compared below with those of the present study.

Mass (1981) used data from rawinsondes and surface stations to study the flow of boundary-layer

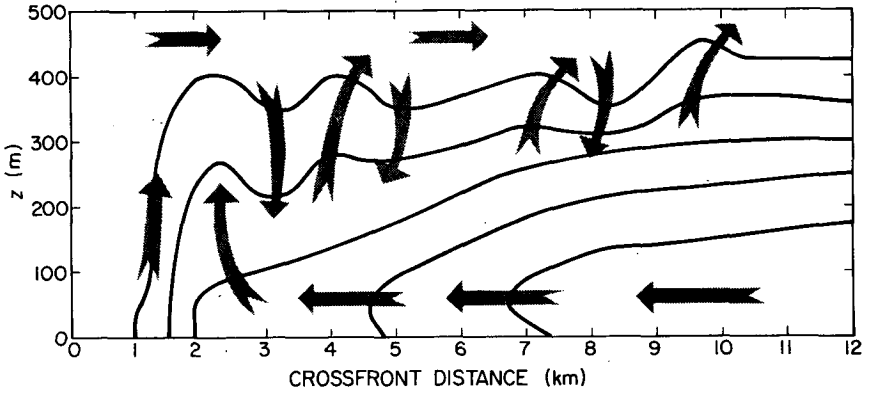

FIG. 10. Schematic representation of micro-α-scale structure and eddies within a cold front head. Solid lines represent scalar isopleths such as wind speed or potential temperature. Arrows represent the flow relative to the surface front.

winds through gaps between the coastal ranges on the west coast of North America. He found that these flows form convergence zones which resemble shallow cold fronts. Mesoscale diabatic forcing was responsible for generating the temperature differences which were observed across the convergence zones. While the 3 December 1981 cold front was of macroscale rather than mesoscale origin, it also exhibited flow around mesoscale obstacles, in this case the higher western end of the Cheyenne Ridge.

Chopra and Hubert (1964, 1965), Lyons and Fujita (1968) and Zimmerman (1969), using satellite images of stratocumulus decks, studied the vortex streets shed by islands. They found that when islands extended up through the capping inversion they acted as obstacles to the boundary-layer flow and shed a series of vortices in the boundary layer. The 3 December 1981 cold front was similar in that flow of a shallow cold air mass was diverted around an obstacle. The height of the ridge was similar to the depth of the cold fluid. However, in the case of the cold front the eddy remained in the immediate lee of the ridge throughout the study period. The existence of an obstacle, the Palmer Lake Divide, located downstream of the Cheyenne Ridge may have served to lock the eddy in position. Alternatively, the large scale of the obstacle may have resulted in an eddy life cycle longer than the study period, so that only the formative stages were observed.

Previous studies of mesoscale and microscale features of cold fronts, including those of Clark (1961), Browning and Harrold (1970), Martin (1973), Carbone (1982), Hobbs and Persson (1982) and Parsons and Hobbs (1983) have used a wide variety of sensors.

Carbone (1982) studied a narrow cold frontal rain band in the central valley of California. Triple-Doppler radar measurements with average data spacing of 300 m were supplemented by upper air soundings and surface measurements of temperature, humidity, pressure and precipitation. The existence of mesoscale eddies at 13 km intervals along the front was related to a Helmholtz-type inflectional instability. A strong low-level jet parallel to and ahead of the front provided the across-front horizontal shear necessary for this instability mechanism. Hobbs and Persson (1982) and Parsons and Hobbs (1983) used Doppler radar, aircraft and surface observations to study narrow cold frontal rain bands along the coast of Washington state. They found that narrow cold frontal rain bands were composed of distinct precipitation cores separated by gap regions. They postulated that the observed low-level jet parallel to and ahead of the fronts lead to these wave-like perturbations in the frontal position by this same Helmholtz inflectional instability mechanism. This phenomenon would not have been reliably detected by the surface network used in the present study. However, the lack of a low-level jet parallel to and ahead of the front in the mesoscale region studied suggests that the Helmholtz inflectional instability mechanism was not active in this case.

This and previous studies describe a variety of mesoscale flow features associated with synoptic-scale cold fronts. Not all of these features are found in all cold fronts.

b. Microscale structures

The studies discussed above also described various microscale structures of cold fronts. There have also been a number of studies of the microscale structure of thunderstorm gust fronts and laboratory gravity currents which are similar in many respects to cold fronts. The methods and results of these studies are compared below with those of the present study.

Frontal updrafts have been found to be a consistent feature of atmospheric gravity currents. Browning and Harrold (1970) used Doppler radar to study air motion and precipitation growth in a moist cold front. They found that the two-dimensional line convection along the cold front was mechanically rather than buoyantly forced. The precipitation fell from the air of the pre-frontal boundary layer as it was lifted over the advancing cold air mass. Updrafts were found to be 8 m s^{-1} and the frontal speed 12 m s^{-1}. For the narrow cold frontal rainband described in the previous subsection, Carbone (1982) found prefrontal updraft speeds of 15–20 m s^{-1} with a frontal speed of 21.7 m s^{-1}. The updraft band was 2–3 km wide and the maximum vertical velocity was at an elevation of 2.1 km, the same level as the top of the cold air mass. The convection associated with this front was also forced rather than buoyant. The narrow cold frontal rainbands studied by Hobbs and Persson (1982) and Parsons and Hobbs (1983) had distinct three-dimensional precipitation cores with updrafts of 3–7 m s^{-1} in bands approximately 2 km wide along their leading edges. While the convection reported by Parsons and Hobbs (1983) was forced as in the cases referred to above, that reported by Hobbs and Persson (1982) was buoyant. In neither study were the precipitation cores found to extend above 4 km. These features of the forced or shallow buoyant moist convection along cold fronts are similar to those found in the 3 December 1981 cold front. On 3 December, updraft speeds at the frontal surface exceeded 6 m s^{-1} with a frontal speed of approximately 10 m s^{-1}. This leading updraft was 0.8 km wide and extended from below 10 m to above the top of the 300 m BAO tower.

The updrafts associated with the leading edges of thunderstorm gust front flows have sizes and magnitudes similar to those reported for cold fronts. However, the presence of an overhanging nose of denser fluid leads to the primary updraft being located ahead of the surface temperature drop. Charba (1974) used data from the KTVY meteorologically-instru-

mented tower to study a thunderstorm gust front. An updraft strength of 2.4 m s^{-1} was reported at an elevation of 400 m for a thunderstorm gust front which had a forward speed of 20 m s^{-1}. This vertical velocity is conservatively small because of the low-pass filtering which had been applied to the tower data. Goff (1976) also used the KTVY meteorologically instrumented tower to study 20 thunderstorm gust fronts. The primary updrafts were found to be approximately 1.5 km wide with vertical velocities in excess of 6 m s^{-1}. Goff (1976) also reported the presence of overhanging noses of denser air ahead of the surface temperature drop.

Charba (1974) reported passage of a thunderstorm gust front as a sequence of temporally distinct phenomena. At the surface, a pressure jump occurred first, followed within one minute by a change in wind direction. More than two minutes later, the gust surge occurred followed by the temperature drop. The overhanging nose of this thunderstorm gust front accounted for much of this temporal separation. The primary updraft, temperature drop, wind-shift and gust surge in the 3 December 1981 dry cold frontal passage occurred within ten seconds. The lack of an overhanging nose in this case contributed to this simultaneity. A gradual wind shift did however precede the actual frontal passage by some minutes. Because overhanging noses of gravity currents are known to collapse periodically (Simpson, 1969), the lack of such a nose on the 3 December 1981 cold front at the BAO tower does not exclude the possibility that such a feature may have existed at other times and locations on this and similar fronts.

Various authors have reported the presence of microscale eddies in the frontal zones of atmospheric and laboratory gravity currents. Simpson (1969) compared laboratory gravity currents with sea breezes and haboobs. Billows were observed to occur in the frontal surface of haboobs and laboratory density currents. The laboratory studies permitted description of the life cycle of these eddies as they formed at the gravity current nose and moved backward to break behind the head. Similar eddies can be seen in the temperature and velocity time–height sections for the 3 December 1981 case. These quasi-periodic perturbations can be seen in Figs. 6–10. Carbone (1982) reports eddies of a 2 km scale to the rear of a moist cold front. These eddies were three dimensional. A split updraft in the cold frontal head caused by the positioning of one of these eddies was depicted in one of the radar cross sections. This updraft structure is quite similar to that seen in the 3 December 1981 cold front. Hobbs and Persson (1982) also found a split updraft with a weak intervening downdraft in the head of a moist cold front.

Clark (1961) used serial pilot balloon radiosondes and aircraft data to study sea-breeze and dry cold fronts during the Australian summer. The observed cross-isentropic flow in the frontal zone was attributed to convergence of turbulent heat flux. Charba (1974) suggested that the cold current overtaking a thunderstorm gust front from behind serves to reinforce the temperature gradient in the frontal zone. This phenomenon would act against the gradient-dissipating effects of eddies embedded in the frontal zone. Carbone (1982), Hobbs and Perrson (1982), Charba (1974) and Goff (1976) all emphasized that for atmospheric gravity currents there is such a current of cold air overtaking the front from behind. This current can be seen in Figs. 6 and 7, centered at a level between 50 and 100 m. This current is located between the surface friction layer and the turbulent layer within the frontal zone.

Goff (1976) reported thunderstorm gust frontal slopes ranging from very shallow up to 75° from the horizontal. Our results fall in the middle of this range, with a 30–40° slope of the nose of the 3 December 1981 dry cold front. In both studies the upper surface of the frontal nose was much steeper than typical macroscale frontal slopes.

This and the previous studies above show that atmospheric gravity currents of all kinds have many features in common. All exhibit considerable structure on the meso- and microscales. Indeed, a significant portion of the transition between macroscale air masses can occur on spatial scales of less than 100 m and time scales of less than 10 s. The existence of such wind gradients within dry cold fronts has serious implications for aviation safety.

5. Conclusions

There exists within cold frontal zones a variety of structures too small to be detected by current synoptic networks. The study of data from the PROFS surface mesonetwork has revealed the flow of a shallow cold front around a terrain obstruction. A meso-β-scale anticyclonic lee eddy eventually formed downwind of this obstruction. The effect of terrain was to channel the cold flow westward up the South Platte River drainage basin resulting in frontal passages from the east and southeast at stations near the foothills of the Front Range. An awareness of this channeling would be quite useful to a meteorologist forecasting frontal passage and associated weather in complex terrain.

Micro-α-scale vertical eddies were observed to mix relatively warm, low momentum air down through the frontal surface as it passed the BAO tower. These eddies correspond to those hypothesized by Martin (1973) to explain his surface observations and to the breaking billows observed in laboratory gravity currents. The 3 December 1981 cold frontal flow consisted of a jet of cold air near the surface which was both diluted by mixing from above and replenished by flow overtaking it from behind.

A large portion of the macroscale temperature and wind changes were found to occur within a micro-α-scale frontal zone. The temperature decrease, wind-shift line and primary updraft core occurred within 10 s of each other, in contrast to the larger temporal separation of these events observed in thunderstorm gust fronts. This difference is due to the presence of an overhanging nose of cold air in the gust fronts, which was lacking in this cold front.

The strong wind shears and microscale turbulence associated with this dry cold front could have presented a hazard to aircraft operating at low levels. These microscale features cannot be resolved by the macroscale network. However, airport low-level wind shear observation systems should be able to detect at least the surface wind-shift line.

Acknowledgments. The authors appreciate the assistance of James Toth and Bonnie Weber of CSU and John Gaynor, Dan Wolfe and other staff of the NOAA BAO in data acquisition. We also thank Machel Sandfort for typing the manuscript and Judy Sorbie for drafting the figures. This work was supported by the Division of Atmospheric Sciences, National Science Foundation under Grant ATM-8206808.

REFERENCES

Anthes, R. A., Ed., 1983: *The National STORM Program—Scientific and Technological Bases and Major Objectives.* Rep. to NOAA, Contract NA81RAC00123, University Corporation for Atmospheric Research, Boulder, CO, 520 pp.

Browning, K. A., and T. W. Harrold, 1970: Air motion and precipitation growth at a cold front. *Quart. J. Roy. Meteor. Soc.*, **96**, 369–389.

Carbone, R. E., 1982: A severe frontal rainband. Part I: Stormwide hydrodynamic structure. *J. Atmos. Sci.*, **39**, 258–279.

Charba, J., 1974: Application of a gravity current model to analysis of a squall-line gust front. *Mon. Wea. Rev.*, **102**, 140–156.

Chopra, K., and L. F. Hubert, 1964: Kármán vortex-streets in the earth's atmosphere. *Nature*, **203**, 1341–1343.

——, and ——, 1965: Mesoscale eddies in the wakes of islands. *J. Atmos. Sci.*, **22**, 652–657.

Clarke, R. H., 1961: Mesostructure of dry cold fronts over featureless terrain. *J. Meteor.*, **18**, 715–735.

Goff, R. C., 1976: Vertical structure of thunderstorm outflows. *Mon. Wea. Rev.*, **104**, 1429–1440.

Hobbs, P. V., and P. O. G. Persson, 1982: The mesoscale and microscale structure and organization of clouds and precipitation in midlatitude cyclones. Part V: The substructure of narrow cold frontal rainbands. *J. Atmos. Sci.*, **39**, 280–295.

Kaimal, J. C., and J. E. Gaynor, 1983: The Boulder Atmospheric Observatory. *J. Climate Appl. Meteor.*, **22**, 863–880.

Lyons, W. A., and T. Fujita, 1968: Meso-scale motions in oceanic stratus as revealed by satellite data. *Mon. Wea. Rev.*, **96**, 304–314.

Martin, H. G., 1973: Some observations of microstructure of dry cold fronts. *J. Appl. Meteor.*, **12**, 658–663.

Mass, C., 1981: Topographically forced convergence in western Washington State. *Mon. Wea. Rev.*, **109**, 1335–1347.

Orlanski, I., 1975: A rational subdivision of scales for atmospheric processes. *Bull. Amer. Meteor. Soc.*, **56**, 527–530.

Parsons, D. B., and P. V. Hobbs, 1983: The mesoscale and microscale structure and organization of clouds and precipitation in midlatitude cyclones. Part XI: Comparisons between observational and theoretical aspects of rainbands. *J. Atmos. Sci.*, **40**, 2377–2397.

Reed, R. J., 1980: Destructive winds caused by an orographically induced mesoscale cyclone. *Bull. Amer. Meteor. Soc.*, **61**, 1346–1355.

Reynolds, D. W., 1983: Prototype workstation for mesoscale forecasting. *Bull. Amer. Meteor. Soc.*, **64**, 264–273.

Simpson, J. E., 1969: A comparison between laboratory and atmospheric density currents. *Quart. J. Roy. Meteor. Soc.*, **95**, 758–765.

Smith, R. B., 1981: An alternate explanation for the destruction of the Hood Canal bridge. *Bull. Amer. Meteor. Soc.*, **62**, 1319–1320.

Tsuchiya, K., 1969: The clouds with the shape of Kármán vortex street in the wake of Cheju Island, Korea. *J. Meteor. Soc. Japan*, **47**, 457–465.

Zimmerman, L. I., 1969: Atmospheric wake phenomena near the Canary Islands. *J. Appl. Meteor.*, **8**, 896–907.